THE JOURNAL OF BIOLOGICAL CHEMISTRY VOL. 289, NO. 1, pp. 251–263, January 3, 2014

Cited2, a Transcriptional Modulator Protein, Regulates Metabolism in Murine Embryonic Stem Cells*

Received for publication, June 27, 2013, and in revised form, November 20, 2013 Published, JBC Papers in Press, November 21, 2013, DOI 10.1074/jbc.M113.497594

Qiang Li[‡], Parvin Hakimi[‡], Xia Liu[§], Wen-Mei Yu[§], Fang Ye[¶‖], Hisashi Fujioka[¶], Syed Raza[‡], Eswar Shankar[¶], Fangqiang Tang[‡], Sally L. Dunwoodie[‡‡], David Danielpour[¶§§], Charles L. Hoppel[§‖], Diana L. Ramírez-Bergeron[§§¶¶], Cheng-Kui Qu[§§§], Richard W. Hanson[‡], and Yu-Chung Yang[‡§§1]**

*From the Departments of [‡]Biochemistry, [§]Medicine, [¶]Pharmacology, and [¶¶]Cardiovascular Medicine, [§§]Cancer Center, and [‖]Center for Mitochondrial Disease, Case Western Reserve University, Cleveland, Ohio 44106, the **Developmental and Stem Cell Biology Division, The Victor Chang Cardiac Research Institute, Darlinghurst, New South Wales 2010, Australia, and the [‡‡]St. Vincent's Clinical School and the School of Biotechnology and Biomolecular Sciences, University of New South Wales, Kensington, New South Wales 2010, Australia*

Background: The function of HIF-1, a master regulator of metabolism, is in part modulated by Cited2. The role of Cited2 in murine embryonic stem cell (mESC) glucose metabolism remains unknown.
Results: Deletion of *Cited2* in mESCs results in impaired mitochondria morphology, reduced glucose oxidation, increased glycolysis, and defective mESC differentiation.
Conclusion: Cited2 coordinates glucose metabolism to regulate mESC differentiation.
Significance: Cited2 is a potential target for metabolic reprogramming in mESCs.

CREB-binding protein (CBP)/p300 interacting transactivator with glutamic acid (Glu) and aspartic acid (Asp)-tail 2 (Cited2) was recently shown to be essential for gluconeogenesis in the adult mouse. The metabolic function of Cited2 in mouse embryonic stem cells (mESCs) remains elusive. In the current study, the metabolism of glucose was investigated in mESCs, which contained a deletion in the gene for Cited2 (*Cited2*$^{\Delta/-}$). Compared with its parental wild type counterpart, *Cited2*$^{\Delta/-}$ ESCs have enhanced glycolysis, alternations in mitochondria morphology, reduced glucose oxidation, and decreased ATP content. Cited2 is recruited to the hexokinase 1 (*HK1*) gene promoter to regulate transcription of *HK1*, which coordinates glucose metabolism in wild type ESCs. Reduced glucose oxidation and enhanced glycolytic activity in *Cited2*$^{\Delta/-}$ ESCs correlates with defective differentiation during hypoxia, which is reflected in an increased expression of pluripotency marker (*Oct4*) and epiblast marker (*Fgf5*) and decreased expression of lineage specification markers (*T*, *Gata-6*, and *Cdx2*). Knockdown of hypoxia inducible factor-1α in *Cited2*$^{\Delta/-}$ ESCs re-initiates the expression of differentiation markers *T* and *Gata-6*. Taken together, a deletion of *Cited2* in mESCs results in abnormal mitochondrial morphology and impaired glucose metabolism, which correlates with a defective cell fate decision.

CREB[2]-binding protein (CBP)/p300 interacting transactivator with glutamic acid (Glu) and aspartic acid (Asp)-tail 2 (Cited2) is a multifunctional protein essential for mouse embryogenesis (1–4). Embryos with a deletion of *Cited2* have defects in multiple organs including the heart, liver, and adrenal glands and do not survive beyond E14.5 (1–4). A knock-out of *Cited2* in mice causes defects in arterial and ventricular septum and outflow tract, which are responsible for embryonic lethality of a *Cited2* gene deletion (1, 3, 4). By interacting with hepatocyte nuclear factor 4α, Cited2 regulates lipid and carbohydrate metabolism in embryos (2). Interestingly, embryos in which the gene for Cited2 has been deleted have no adrenal gland (1). In adult mice, hematopoietic stem cells are metabolically inactive, as evidenced by cell quiescence, whereas the maintenance of hematopoietic stem cells is sensitive to changes in the metabolism of glucose and fatty acids (5, 6). Importantly, we and others have shown that Cited2 regulates quiescence and apoptosis in adult hematopoietic stem cells via HIF-1 and p53-dependent mechanisms (7, 8). Recently, by adenovirus-mediated delivery of Cited2 small hairpin RNA (shRNA) to mouse hepatocytes, it was demonstrated that Cited2 regulates gluconeogenesis by interacting with histone acetyltransferase GCN5 to affect acetylation and activity of peroxisome proliferative-activated receptor γ co-activator 1α (PGC-1α) (9).

Although Cited2 has been suggested as a crucial player in the regulation of gluconeogenesis, the role of Cited2 in glucose metabolism, especially glycolysis and oxidation phosphorylation in murine embryonic stem cells (mESC) remains elusive. The gene for *Cited2* is present on chromosome 6q.23, a chromosomal region that is associated with genes involved in the control of insulin concentrations and insulin resistance in Mexican-Americans (10, 11). Indeed, *Cited2* mRNA was down-reg-

* This work was supported, in whole or in part, by National Institutes of Health Grants R01HL091896 (to Y-C. Y) and R01HL096597 (to D. R. B.), Grant AG-SS 2420-10 from the Ellison Medical Foundation (to R. W. H.), and National Health and Medical Research Council (NHMRC) Senior Research Fellowship 1042002 (to S. L. D).

[1] To whom correspondence should be addressed: Dept. of Biochemistry and Cancer Center, Case Western Reserve University School of Medicine, 10900 Euclid Ave., W444, Cleveland, OH 44106. Tel.: 216-368-6931; Fax: 216-368-3419; E-mail: yu-chung.yang@case.edu.

[2] The abbreviations used are: CREB, cAMP-response element-binding protein; mESC, murine embryonic stem cell; HIF, hypoxia inducible factor; EB, embryoid body; LDH, lactate dehydrogenase; FCCP, *p*-trifluoromethoxy carbonyl cyanide phenylhydrazone; TCA, tricarboxylic acid; 2-DG, 2-deoxy-glucose; TMRM, tetramethylrhodamine methyl ester; OCR, oxygen consumption; HK, hexokinase; PFK1, phosphofructokinase 1; CFU, colony formation unit.

ulated by insulin in skeletal muscle of 17 healthy volunteers exposed to acute physiological hyperinsulinemia (10). In contrast, *Cited2* mRNA was one of the top five up-regulated transcripts in 8 Type 2 diabetics, as compared with 8 non-diabetic subjects after low-dose insulin infusion (12). These studies strongly suggest that Cited2 plays an important role in insulin-mediated signaling pathways that regulate glucose metabolism in humans.

ESCs represent a unique cell population that are characterized by their small size, rapid proliferation, and resistance to senescence, which provides a robust platform for metabolic studies (13). In the undifferentiated state, the majority of glucose (80%) enters the glycolytic pathway to maintain ESC proliferation and self-renewal (14, 15). Lin-28 and c-Myc, two proteins that determine ESC pluripotency, also regulate glucose metabolism, suggesting a possible connection between the rate of glucose utilization and ESC self-renewal (16–18). Moreover, metabolic fluctuations exist at different time points of ESC differentiation. In the early stages of differentiation into epiblast stem cells, 98% of glucose is consumed for lactate production (14). At mid-to-late differentiation, ESCs undergo a metabolic switch from glycolysis to mitochondrial oxidative phosphorylation to provide sufficient ATP for differentiation (19, 20). A metabolic switch from oxidative phosphorylation to glycolysis would thus favor reprogramming of terminally differentiated mouse fibroblasts to induced pluripotent stem cells (21). Although the metabolic dynamics is critical for proper ESC differentiation, little is known about how ESC pro-differentiation factors modulate glucose homeostasis during this process.

Cited2 was recently characterized as a pro-differentiation factor in the mouse ESCs (22, 23). In this study, we report that mESCs with a deletion in the gene for *Cited2* (*Cited2*$^{\Delta/-}$) have swollen mitochondria, increased mitochondrial number, and reduced mitochondrial function as reflected by a reduced rate of glucose oxidation. Impaired glucose oxidation and increased glycolytic activity in *Cited2*$^{\Delta/-}$ ESCs is associated with defective differentiation during hypoxia. In particular, *Cited2*$^{\Delta/-}$ ESCs display increased mRNA expression of pluripotency marker (*Oct4*) and epiblast marker (*Fgf5*), and defective mRNA induction of lineage markers (*T*, *Gata-6*, and *Cdx2*). Knockdown of hypoxia inducible factor (HIF)-1α in *Cited2*$^{\Delta/-}$ ESCs re-initiates expression of lineage markers *T* and *Gata-6*. Furthermore, Cited2 is recruited to the *HK1* gene promoter to directly modulate the expression of *HK1*, a key enzyme in glycolysis. Thus, Cited2 coordinates glucose metabolism, pluripotency, differentiation, and cell proliferation and is a potential target for metabolic reprogramming in ESCs.

EXPERIMENTAL PROCEDURES

ES Cell Culture and Induced Differentiation—*Cited2*$^{Flox/+}$ (hereafter referred to as wild type, WT) and *Cited2*$^{\Delta/-}$ ESC (clone number 3) were utilized for most of the experiments performed in this study. To maintain ESCs under undifferentiated status in feeder-free culture system, WT and *Cited2*$^{\Delta/-}$ ESCs stably transfected with Oct4-IRES-GFP-Puro^{R} reporter plasmid were grown on gelatin-coated plates in complete ESC media (DMEM (Invitrogen) containing 25 mM glucose, 15% ES-qualified FBS (Germini), 2.5 mM Glutamax (Invitrogen), 1× non-essential amino acids (Invitrogen), 55 μM 2-mercaptoethanol (Invitrogen), and 1,000 IU/ml of ESGRO® leukemia inhibitory factor (Millipore)). ESCs were periodically selected with puromycin to maintain a population of undifferentiated ESC. ESCs were induced to differentiate via a methylcellulose-based method as described previously (22). For hypoxia experiments, ESCs were cultured or induced to differentiate in an incubator with an adjustable oxygen concentration, as described elsewhere (24).

Measurement of Glucose, Lactate, Glycolytic Activity, and Cell Proliferation—Undifferentiated ES cells were cultured in 0.1% gelatin-coated dishes and media was collected at the indicated time points for measurement of glucose and lactate, as described elsewhere (25–27). For primary embryoid bodies (EB) that were differentiating in methylcellulose-based semi-solid media, the EBs were re-suspended at 37 °C in PBS and centrifuged at 300 × *g* for 5 min. The supernatant was diluted 10-fold for the measurement of glucose and lactate via spectrophotometric methods. For glucose measurement, the sample was mixed with trithanolzmine buffer containing $MgSO_4$, ATP/NADP, and Glc-6-PDH to record initial absorbance at 340 nm. Hexokinase solution was then added and the final absorbance was read when the absorbance was stabilized for 15 s. The absorbance difference was used for the calculation of glucose concentration. For lactate measurement, the sample was mixed with hydrazine/glycine buffer and NAD solution in a test tube and extinction E1 at 340 nm was recorded. After adding lactate dehydrogenase (LDH), the mixture was incubated at 37 °C for 30 min and the extinction E2 was determined. Extinction difference between E1 and E2 was then used to calculate lactate concentration. The relative percentage of glucose metabolized to lactate was utilized for the assessment of glycolytic activity (relative glucose conversion to lactate = [lactate production (μmol)]/[2× glucose consumption (μmol)] × 100%). Cell proliferation was assessed by a CellTiter 96® AQueous One Solution Cell Proliferation Assay (Promega).

Oxidation of Glucose, Acetate, and Glutamate to Carbon Dioxide—The oxidation of [U-^{14}C]-glucose, [2-^{14}C]acetate, and [U-^{14}C]glutamate to $^{14}CO_2$ was determined as previously described (28). In brief, 1–6 × 10^6 cells were resuspended in 2 ml of DMEM (11966-025, Invitrogen) in a flask that contained [U-^{14}C]glucose (5 mM, 0.5 μCi), [2-^{14}C]acetate (1 mM, 0.5 μCi), or [U-^{14}C]glutamate (1 mM, 0.5 μCi) and incubated at 37 °C for 4 h. The experimental procedures and device used for release of $^{14}CO_2$ trapping were described elsewhere (28).

Electron Microscopy (EM)—Undifferentiated ESCs (5 × 10^4 cells) were seeded on gelatin-coated, 12-well plates and cultured for 2 days. Cells were fixed immediately with a triple aldehyde-dimethyl sulfoxide fixative and processed by the Case Western Reserve University School of Medicine Electron Microscopy Core Facility.

ATP Measurement—The total ATP content of ESCs was determined by using an adenosine 5′-triphosphate bioluminescent somatic cell assay kit (Sigma) as described elsewhere (29).

Oxygen Consumption Assay—ESC oxygen consumption was determined using the Seahorse® XF-24 Bioanalyzer and Oxgraph-2K®-based platform. For the Seahorse XF-24-based assay, 120,000 undifferentiated ESCs were seeded on Cel-Tek®

(BD)-coated XF-24 plates for 1 h. The assays were performed in the unbuffered XF-24 assay media in the presence of 25 mM glucose, 2.5 mM pyruvate, and 2 mM L-alanyl-glutamine (Glutamax). The rate of oxygen consumption at the basal level and upon treatment with oligomycin, *p*-trifluoromethoxy carbonyl cyanide phenylhydrazone (FCCP), or rotenone was recorded sequentially. Respiration by ESCs was determined using an Oxygraph-2K®-based workshop (OROBOROS, Innsbruck, Austria) by re-suspending cells in MiR05 respiration buffer (20 mM HEPES, 10 mM KH_2PO_4, 110 mM sucrose, 20 mM taurine, 60 mM K-lactobionate, 0.5 mM EGTA, 3 mM $MgCl_2$, 0.1% fatty acid-free BSA) (30) at the cell density of 1×10^6/ml. Prior to permeabilization, the basal level of oxygen consumption was monitored and the cells were then permeabilized with digitonin and different mitochondrial respiration substrates were added sequentially to determine the level of oxygen consumption (31). Total protein mass determined by a Bradford assay (Fisher) was used for the normalization of the oxygen consumption rate as described previously (32).

Flow Cytometry—A MitoPT™ TMRM assay kit (ImmunoChemistry Technologies) was used to determine the mitochondria membrane potential. The level of the reduced form of reactive oxidative species in mitochondria was determined by MitoTracker® Orange CM-H2TMRos staining (Invitrogen, catalogue number M7511). Cells were incubated with TMRM (20 nM) or CM-H2TMRos (100 nM) at 37 °C for 30 min in the dark and subjected to analysis using a flow cytometer LSR-II (BD Biosciences).

Genomic DNA Extraction, RNA Isolation, and Quantitative Real-time PCR—Genomic DNA was extracted using ArchivePure DNA cell/tissue kit (5 PRIME GmbH) and RNA was eliminated by RNase treatment. TRIzol® reagent (Invitrogen) was used for RNA isolation. One μg of the isolated RNA was reverse transcribed to cDNA using a High Capacity RNA-to-cDNA Kit (Applied Biosystems) and SYBR Green-based real-time PCR (Roche Applied Science) was performed using a Bio-Rad PCR cycler. Primer sequences used for this study are available upon request.

Lentivirus Production and HIF-1α shRNA Knockdown—293T cells were co-transfected with pLKO-based GFP or with a HIF-1α shRNA plasmid (33) and viral packaging and envelope plasmids, using calcium phosphate-mediated gene delivery to produce lentivirus. After 72 h of incubation, the lentivirus supernatant was filtered and used for infection of ESCs. Stable cell lines with a knockdown of HIF-1α in ESCs were obtained by puromycin selection and validated with real-time PCR and Western blot assays.

Western Blot—Undifferentiated ESCs (5×10^5 cells) were seeded on gelatin-coated 12-well plates. After overnight incubation, cells were replenished with complete ESC media or Hanks' balanced salt solution for 6 h. Cell lysates were harvested with RIPA buffer in the presence of a protease inhibitor mixture (eComplete, Roche Applied Science). Western blots were probed with antibodies to LC3 and p62 (Cell Signaling).

Chromatin Immunoprecipitation (ChIP) Assay—ChIP assay was performed by following a standard protocol (34). Briefly, protein-DNA complexes in WT ESCs were cross-linked with 1% paraformaldehyde and chromatins were sonicated to the average length of 300–500 base pairs. Chromatins were further immunoprecipitated with IgG or CITED2 antibody (R&D Systems) and the enrichment of CITED2 on the hexokinase 1 promoter region was determined by quantitative PCR and normalized to the IgG control (set as 1.0). The four regions randomly selected on the HK1 promoter were: R2, −2502 to −2284; R3, −1655 to −1452; R6, −831 to −609; and R7, −472 to −365 (all are relative distance to transcription start site of the HK1 gene).

Statistical Analysis—Student's *t* test was used to compare the difference between two groups. $p < 0.05$ is considered as a statistically significant difference.

RESULTS

Enhanced Aerobic Glycolysis and Reduced Glucose Oxidation in Undifferentiated Cited2$^{\Delta/-}$ ESCs—Media in the three independent *Cited2*$^{\Delta/-}$ ESC clones previously generated via homologous recombination was noted to become acidic during EB-induced differentiation, as compared with the WT counterpart, suggesting that deletion of *Cited2* may affect the rate of glucose conversion to lactate in ESCs. To gain insights into differential glucose metabolism between WT and *Cited2*$^{\Delta/-}$ ESCs, glucose consumption and the conversion of glucose to lactate and carbon dioxide were measured. During 3 h of incubation, ESCs with *Cited2* deletion consumed ~20% more of glucose (Fig. 1*A*) and consequently produced ~30% more lactate (Fig. 1*B*). Besides conversion to lactate by LDH, glucose-derived pyruvate can be oxidized in the mitochondria to acetyl-CoA by the pyruvate dehydrogenase complex, which can then be oxidized to CO_2 in the tricarboxylic acid (TCA) cycle. Compared with WT ESCs, undifferentiated *Cited2*$^{\Delta/-}$ ESCs oxidized 75% less glucose to carbon dioxide (Fig. 1*C*). Unlike HEK293 cells (positive control), WT and *Cited2*$^{\Delta/-}$ ESCs had a minimal capacity to oxidize [2-^{14}C]acetate to carbon dioxide (Fig. 1*D*). [U-^{14}C]Glutamate also used a substrate to determine the rate of oxidation of 5-carbon intermediates in the TCA cycle. When [U-^{14}C]glutamate was provided in glucose-free DMEM, glutamate oxidation was barely detectable in WT and *Cited2*$^{\Delta/-}$ ESCs (Fig. 1*E*). In addition, the ATP content was reduced by ~30% in *Cited2*$^{\Delta/-}$ ESCs (Fig. 1*F*). These results show that WT and *Cited2*$^{\Delta/-}$ ESCs have a differential capacity to metabolize glucose during short incubation periods, suggesting a role of Cited2 in controlling glucose metabolism in mESCs.

Mouse ESCs possess bivalent metabolic traits (glycolysis and oxidative phosphorylation) to regulate pluripotency, proliferation, and differentiation (35). Because *Cited2* deletion did not affect pluripotency in undifferentiated ESCs from our previous study (22), we tested whether enhanced glycolysis in *Cited2*$^{\Delta/-}$ ESCs supports ESC proliferation and survival. Cell proliferation was similar in WT and *Cited2*$^{\Delta/-}$ESCs during 48 h of incubation, whereas *Cited2*$^{\Delta/-}$ ESCs had modestly increased cell proliferation at 72 h of incubation compared with WT control (Fig. 1*G*). In 48 h of sustained culture (starting cell density: 6202 cells/cm^2/ml), *Cited2*$^{\Delta/-}$ ESCs consumed significantly more glucose (35.57 ± 2.49 *versus* 27.80 ± 2.22 μmol, $p < 0.05$) and produced more lactate (68.33 ± 5.10 *versus* 48.09 ± 3.54 μmol, $p < 0.05$), when compared with WT cells. Because one molecule of glucose is converted to two molecules of lactate during glycolysis, glycolytic activity in WT and *Cited2*$^{\Delta/-}$ ESCs was

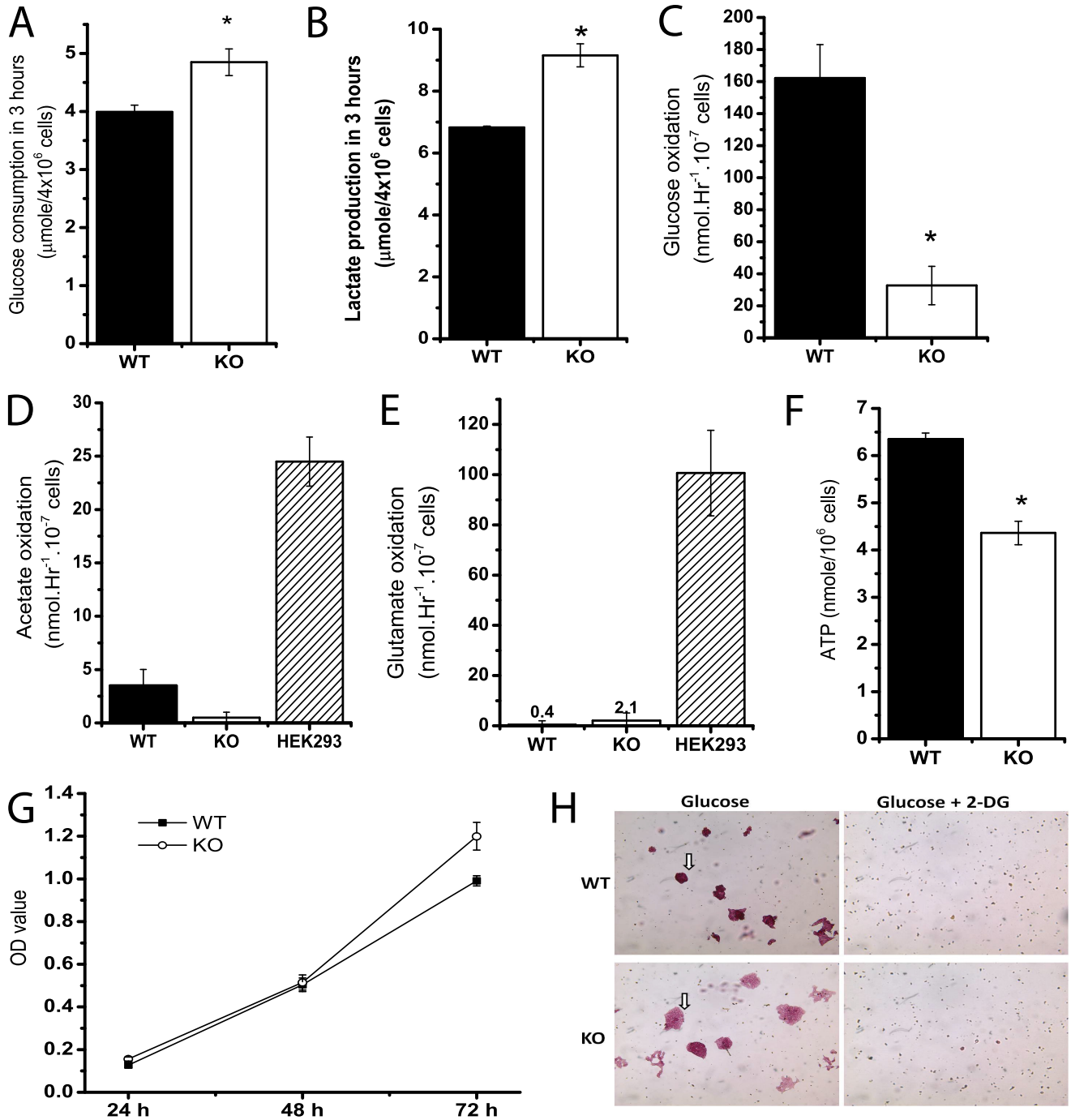

FIGURE 1. **Undifferentiated *Cited2*$^{\Delta/-}$ ESCs have an increased rate of aerobic glycolysis and reduced glucose oxidation.** *A* and *B*, glucose consumption and lactate production in undifferentiated WT and *Cited2*$^{\Delta/-}$ ESCs. 4×10^6 ESCs were resuspended in 2.0 ml of DMEM for 3 h and media were collected for determination of glucose consumption (*A*) and lactate production (*B*), $n = 3$. *C–E*, oxidation of glucose, acetate, and glutamate was measured in undifferentiated WT and *Cited2*$^{\Delta/-}$ ESCs. Undifferentiated ESCs were resuspended in 2.0 ml of DMEM containing [U-^{14}C]glucose (*C*), [2-^{14}C]acetate (*D*), and [U-^{14}C]glutamate (*E*), respectively. The $^{14}CO_2$ release during 4 h of incubation was determined. HEK293 cells were used as a positive control for the oxidation of acetate and glutamate, $n = 3–4$. *F*, the ATP content of WT and *Cited2*$^{\Delta/-}$ ESCs grown in complete ESC media was determined using a firefly luciferase-based assay and further normalized by the cell number, $n = 4$. *G*, proliferation of WT and *Cited2*$^{\Delta/-}$ ESCs. 7,500 cells were seeded on gelatin-coated 96-well plates in 5 replicates and 20 μl of 3-(4,5-dimethylthiazol-2-yl)-5-(3-carboxymethoxyphenyl)-2-(4-sulfophenyl)-2*H*-tetrazolium (inner salt)/phenazine methosulfate solution was added to each well at the indicated time points. Absorbance at 490 nm was recorded and data from two independent experiments are presented. *H*, effect of 2-DG treatment on survival of undifferentiated WT and *Cited2*$^{\Delta/-}$ ESCs. ESCs were seeded on 0.1% gelatin-coated 6-well plates with or without 2-DG. The starting concentration of glucose and 2-DG was 10 and 1 mM, respectively. 72 h later, cells were fixed with 1% paraformaldehyde and subjected to alkaline phosphatase staining. Note that WT and KO ESCs formed colonies with positive AP staining (in *arrows*) in glucose media and no ESC colonies survived by 2-DG treatment. *, $p < 0.05$ compared with WT controls.

evaluated by the relative percentage of glucose converted to lactate (μmol/μmol). During 48 h of incubation, the majority (86.8 ± 1.3%) of glucose consumed was converted to lactate in WT ESCs, whereas *Cited2*$^{\Delta/-}$ ESCs had a significantly greater glycolytic activity (96.1 ± 3.1% of glucose was converted to lactate). In agreement with undifferentiated ESCs tightly

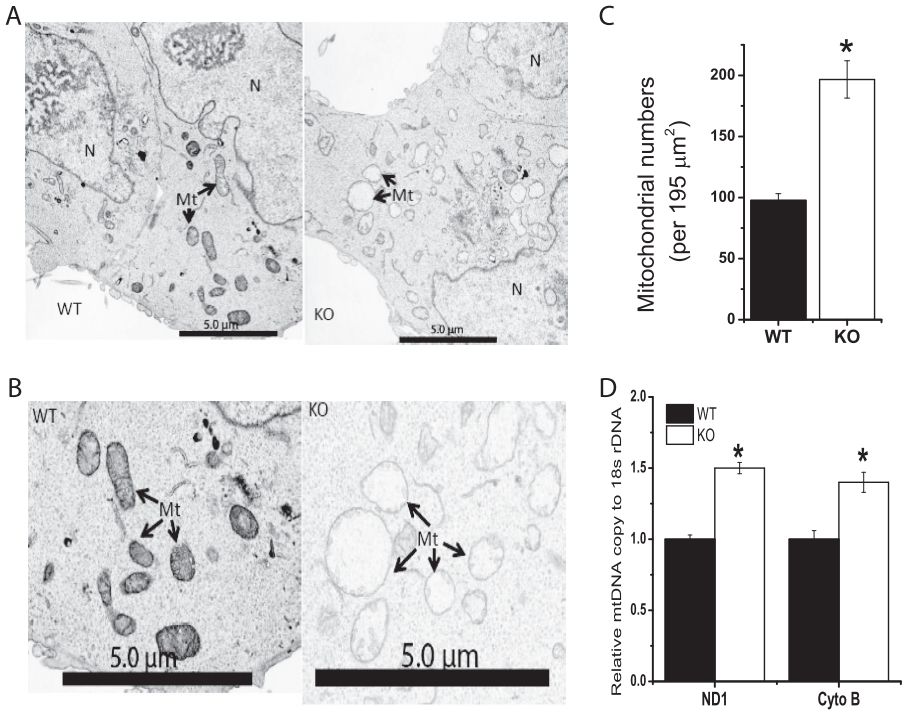

FIGURE 2. ***Cited2*$^{\Delta/-}$ ESCs have abnormal mitochondrial morphology and number.** *A* and *B*, representative electron microscopic images of WT and *Cited2*$^{\Delta/-}$ ESCs at low (*A*) and high (*B*) magnification were presented. *Mt*, mitochondria. *N*, nucleus. *Black scale bar*, 5.0 μm. *C*, the number of mitochondria in WT and *Cited2*$^{\Delta/-}$ ESCs. Mitochondrial number was determined from four individual EM electron microscopic images with ×2000 magnification. *D*, mitochondrial DNA copy in WT and *Cited2*$^{\Delta/-}$ ESCs determined by quantitative PCR. Genomic DNA was extracted from ESCs and relative copy of mitochondrial DNA (NADH dehydrogenase 1, *ND1*, and cytochrome *b, Cyto B*) was normalized by nuclear DNA (*18S* rDNA). Data from two independent experiments are presented. *, $p < 0.05$ compared with WT controls.

dependent on aerobic glycolysis for maintaining survival and pluripotency (15), WT and *Cited2*$^{\Delta/-}$ ESCs treated with specific glycolysis inhibitor 2-deoxyglucose (2-DG) were not able to retain undifferentiated colonies with positive alkaline phosphatase (AP) staining (Fig. 1*H*). Collectively, these data demonstrate that *Cited2*$^{\Delta/-}$ ESCs display enhanced aerobic glycolysis and reduced glucose oxidation, and that alternations in glucose metabolism in undifferentiated *Cited2*$^{\Delta/-}$ ESCs did not affect ESC pluripotency and proliferation.

Cited2$^{\Delta/-}$ *ESCs Have Altered Morphology and an Increase in the Number of Mitochondria*—A reduced rate of glucose oxidation by *Cited2*$^{\Delta/-}$ ESCs suggested that mitochondrial functions might be affected in these cells. We next compared the ultrastructure of WT and *Cited2*$^{\Delta/-}$ ESCs by EM. WT ESCs had a low number of mitochondria with typical morphology, which is consistent with previous reports (36) (Fig. 2, *A* and *B*). Interestingly, swollen mitochondria and an increased number of mitochondria were found in *Cited2*$^{\Delta/-}$ ESCs (Fig. 2, *A*–*C*). The ratio of total mitochondrial DNA (mtDNA) copy to nuclear DNA copy reflects mitochondrial content. The increased mitochondrial number parallels the higher ratio of the mtDNA copy (*ND1* and cytochrome *b*) to nuclear DNA (*18S* rDNA) copy in *Cited2*$^{\Delta/-}$ ESCs (Fig. 2*D*). Swollen mitochondria are associated with reduced mitochondrial membrane potential, increased apoptosis, accumulated ROS in the mitochondria, and are defective autophagy in multiple cell types (37–40). To test whether the mitochondrial membrane potential is affected by abnormal morphology, we performed tetramethylrhodamine methyl ester (TMRM) staining and found that mitochondrial membrane potential was increased by ~20% in *Cited2*$^{\Delta/-}$ ESCs (Fig. 3*A*). The increased TMRM staining of *Cited2*$^{\Delta/-}$ ESCs and comparable basal apoptosis in WT and *Cited2*$^{\Delta/-}$ ESCs (22) suggests that the swollen mitochondria in *Cited2*$^{\Delta/-}$ ESCs are independent of apoptosis. Furthermore, WT and *Cited2*$^{\Delta/-}$ ESCs had comparable levels of the reduced form of ROS in their mitochondria (Fig. 3*B*), indicating that ROS is not the main contributor for the swollen mitochondria in these cells. Swollen mitochondria are associated with accumulated ubiquitin and mitophagy markers, such as LC3 and p62/SQSTM1 (39, 40). In complete ESC media, *Cited2*$^{\Delta/-}$ ESCs had increased conversion of LC3-I into LC3-II, the lipidated form of LC3, whereas p62 protein expression was comparable in WT and *Cited2*$^{\Delta/-}$ ESCs (Fig. 3*C*). Upon nutrient deprivation, *Cited2*$^{\Delta/-}$ ESCs not only had an increased rate of conversion of LC3-I into LC3-II but also an accumulation of p62 protein (Fig. 3*C*). Taken together, *Cited2*$^{\Delta/-}$ ESCs display altered mitochondrial morphology and number, which is associated with a reduced rate of glucose oxidation, increased mitochondrial membrane potential, and impaired autophagy.

Cited2$^{\Delta/-}$ *ESCs Have an Enhanced Oxygen Consumption Capacity*—Because we observed reduced glucose oxidation, swollen mitochondria, and an increased number of mitochondria in *Cited2*$^{\Delta/-}$ ESCs, we tested whether these alternations are coupled with oxygen consumption. The rate of basal oxygen consumption (OCR) was comparable for adherent WT and *Cited2*$^{\Delta/-}$ ESCs in the media containing 25 mM glucose, 2.5 mM pyruvate, and 2 mM L-alanyl-glutamine (Glutamax) (Fig. 3*D*). OCR was blocked by the ATP synthase inhibitor oligomycin to

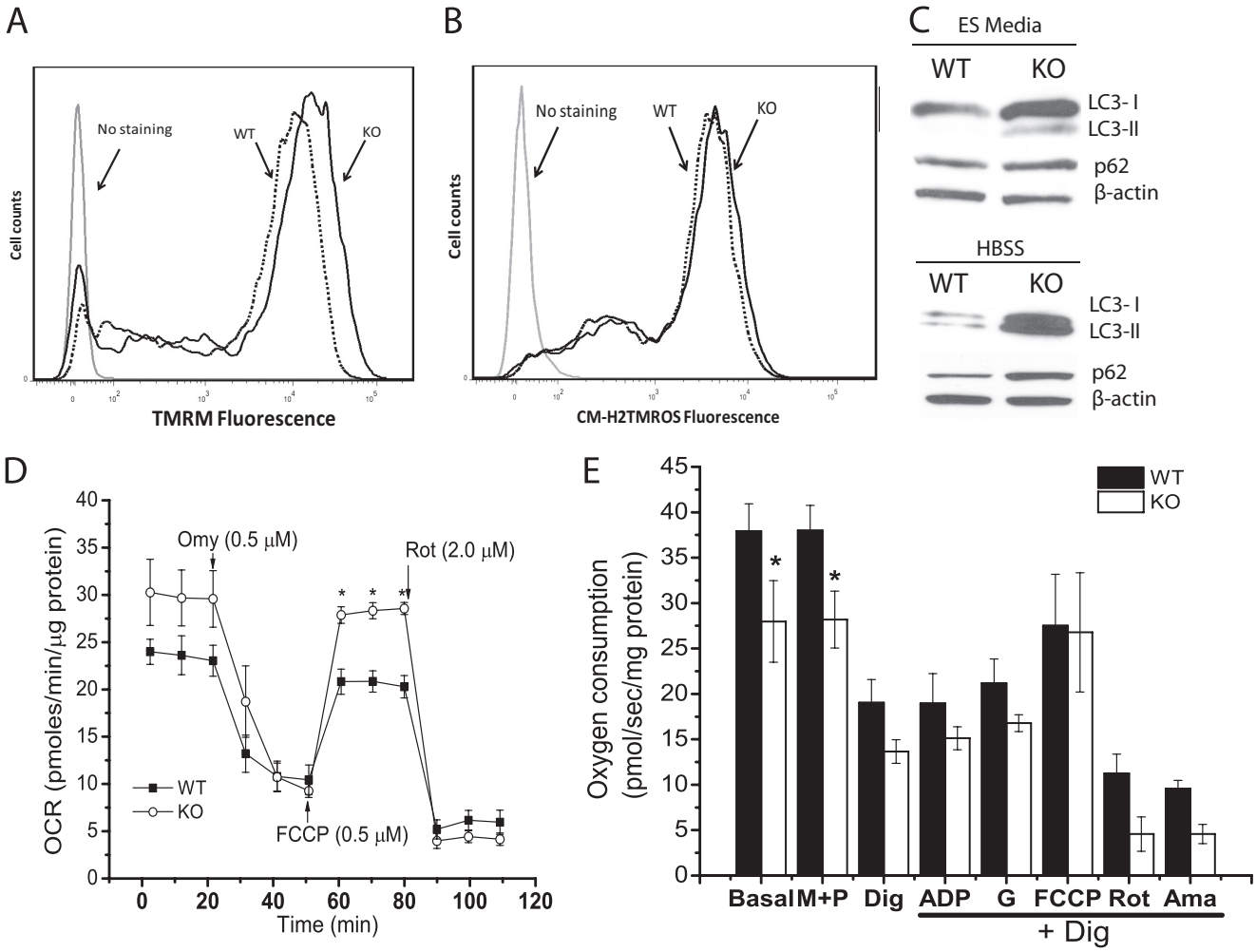

FIGURE 3. **Mitochondrial membrane potential, ROS production, autophagy induction and oxygen consumption in WT and *Cited2*$^{\Delta/-}$ ESCs.** *A,* the mitochondrial membrane potential was measured by TMRM staining through flow cytometry and representative data are presented. *Dashed line*, WT ESCs; *solid line, Cited2*$^{\Delta/-}$ ESCs. *B,* the levels of the reduced forms of mitochondrial ROS were determined by MitoTracker Orange CM-H2TMRos staining and representative data are presented. *Dashed line*, WT ESCs; *solid line, Cited2*$^{\Delta/-}$ ESCs. *C,* conversion of LC3-I into LC3-II and p62 protein expression in WT and *Cited2*$^{\Delta/-}$ ESCs. Cells were grown in complete ESC media and upon nutrient deprivation (in Hanks' balanced salt solution for 6 h) proteins were isolated and analyzed by Western blot assay. *D,* respiration of intact ESC mitochondria was determined using a Seahorse XF-24-based platform. WT and *Cited2*$^{\Delta/-}$ ESCs (1.2×10^5/well) were attached to a XF-24 plate in non-buffered assay media (containing 25 mM glucose, 2 mM L-alanyl-glutamine, and 2.5 mM sodium pyruvate). The OCR at basal, and upon sequential injection of oligomycin, FCCP, or rotenone was recorded and normalized by total protein mass. The experiment was repeated 4 times independently and one set of representative data are presented. *E,* the respiration of mitochondria was monitored in permeabilized ESCs by Oxygraph-2K-based workshop. ESCs were re-suspended in MiR05 buffer at a density of 1×10^6/ml. Prior to permeabilization, oxygen consumption at the basal level, and after stimulating with malate (*M*, 2 mM) and pyruvate (*P*, 2.5 mM), cells were then permeabilized with digitonin (*Dig*, 2.5 μg/ml) and oxygen consumption was recorded. After permeabilization, the substrates indicated in the figure were added sequentially to determine the level of oxygen consumption. ADP, 2.5 mM. *G*, glutamate (10 mM). FCCP, 0.75 μM. *Rot*, rotenone (0.125 μM). *Ama*, antimycin (0.2 μM). The data are normalized by total protein mass and presented as mean ± S.E. of 3 independent experiments. *, $p < 0.05$ compared with WT controls.

a similar extent in WT and *Cited2*$^{\Delta/-}$ ESCs. In the presence of 0.5 μM FCCP, *Cited2*$^{\Delta/-}$ ESCs exhibited modestly increased OCR as compared with WT control cells, indicating that *Cited2*$^{\Delta/-}$ ESCs retained enhanced oxygen consumption capacity. Upon rotenone treatment, OCR was similarly inhibited in WT and *Cited2*$^{\Delta/-}$ ESCs; thus the enhanced capacity for oxygen consumption correlates with the increased mitochondrial number and membrane potential observed in *Cited2*$^{\Delta/-}$ ESCs, whereas oxygen consumption in swollen mitochondria is independent of reduced glucose oxidation observed in *Cited2*$^{\Delta/-}$ ESCs.

To further monitor mitochondrial respiration mediated by different substrates and inhibitors in permeabilized ESCs, we utilized Oxygraph-2K to measure ESC oxygen consumption in the MiR05 buffer. Compared with WT control, basal oxygen consumption of *Cited2*$^{\Delta/-}$ ESCs in the MiR05 mitochondria buffer was reduced (Fig. 3*E*), whereas maximal mitochondrial respiration capacity upon FCCP treatment was also enhanced in intact *Cited2*$^{\Delta/-}$ ESCs, as compared with the WT control cells (data not shown). Digitonin-mediated cellular permeabilization resulted in ~50% reduction in OCR in WT and *Cited2*$^{\Delta/-}$ ESCs, reflecting the typical response to endogenous ADP depletion by digitonin. The addition of ADP and glutamate did not stimulate oxygen consumption in WT and *Cited2*$^{\Delta/-}$ ESCs, whereas FCCP treatment of permeabilized ESCs caused only a ~20% increase in mitochondrial respiration in both groups (Fig. 3*E*). Interestingly, WT and *Cited2*$^{\Delta/-}$ ESCs had a ~50% reduction of OCR in the presence of rotenone, an

inhibitor of Complex I of the respiratory chain, indicating that both ESCs maintain mitochondrial respiration. Collectively, intact *Cited2*$^{\Delta/-}$ ESCs have modestly increased oxygen consumption compared with the WT control, whereas permeabilized WT and *Cited2*$^{\Delta/-}$ ESCs do not respond to ADP stimulation, yet remain sensitive to rotenone inhibition of oxygen consumption.

Cited2 Regulates Expression of Metabolism-associated Genes in Undifferentiated ESCs—Because undifferentiated *Cited2*$^{\Delta/-}$ ESCs exhibited enhanced aerobic glycolysis, we investigated whether glycolysis associated genes are affected in these cells. The activity of LDH is known to be elevated during mouse embryonic development from the one-cell stage to blastocyst formation (embryonic day 0 to 3–4), whereas there is an increase in the activity of hexokinase (HK) (14). Glycogen synthase activity is decreased during embryonic day 3–4, whereas phosphofructokinase 1 (PFK1) activity remains the same during embryonic development to blastocysts (14). We determined mRNA transcripts of *HK* (1 to 4 isoforms), *PFK1* (liver (L) and muscle (M) isoforms), pyruvate kinase (*PK*), LDH (A to D isoforms) in *Cited2*$^{\Delta/-}$ and reconstituted *Cited2*$^{\Delta/-}$ ESCs by stably transfected with Cited2 expression plasmid. We have previously shown that Cited2 regulates *Oct4* gene expression in ESCs (14). It is therefore not surprising that expression of the gene for *HK1*, an Oct4 target gene (41), was reduced to 1.6-fold in reconstituted *Cited2*$^{\Delta/-}$ ESCs (Fig. 4*A*). PFK1 is a rate-limiting enzyme in glycolysis; we noted that mRNA for *PFK1-L*, but not *PFK1-M* was increased to 2-fold in reconstituted *Cited2*$^{\Delta/-}$ ESCs (Fig. 4*A*). In addition, the mRNA for *PK*, another key regulatory enzyme in glycolysis was not affected in reconstituted *Cited2*$^{\Delta/-}$ ESCs (Fig. 4*A*). LDHB is a major regulator of glycolysis in normal and cancer cells (42–44) and *LDHB* mRNA was not changed in reconstituted *Cited2*$^{\Delta/-}$ ESCs (Fig. 4*A*). Furthermore, reintroduction of Cited2 significantly enhanced the reduced level of glucose oxidation in *Cited2*$^{\Delta/-}$ ESCs (Fig. 4*B*). The direct role of Cited2 in the regulation of *HK1* gene transcription was further evidenced by ~5-fold enrichment by Cited2 antibody against IgG control on the R3 region of the HK1 promoter (Fig. 4*C*), with modest enrichment in the R7 region and no enrichment in the R2 and R6 regions of the *HK1* gene promoter (Fig. 4*C*). Collectively, Cited2 is recruited to the *HK1* gene promoter to directly control *HK1* gene expression and regulate glucose metabolism.

Increased Glycolytic Activity and Impaired Hypoxic Differentiation in Cited2$^{\Delta/-}$ *ESCs*—Because glucose metabolism was altered by *Cited2* deletion but did not affect mESC pluripotency and proliferation in undifferentiated ESCs, we further explored whether enhanced glycolysis and reduced glucose oxidation caused by *Cited2* deletion impact ESC differentiation. During ESCs differentiating to cardiomyocytes, the rate of lactate production, normalized by time and total protein mass was reported to be reduced to 2-fold, supporting the notion that metabolic reprogramming is essential for proper ESC differentiation (19). We previously demonstrated that *Cited2*$^{\Delta/-}$ ESCs exhibit defective cardiomyocyte and hematopoietic differentiation during normoxia (22). In WT and *Cited2*$^{\Delta/-}$ EBs favoring cardiomyocyte differentiation, glucose oxidation was reduced by 30% in *Cited2*$^{\Delta/-}$ EBs compared with the WT control (Fig. 5*A*), indicating *Cited2*$^{\Delta/-}$ EBs retain defects in glucose oxidation in both undifferentiated and differentiating *Cited2*$^{\Delta/-}$ ESCs. To test whether differentiating *Cited2*$^{\Delta/-}$ ESCs have changes in glycolysis as ESCs in the undifferentiated state, we took advantage of ESC differentiation during hypoxia based on two considerations. First, hypoxia supports ESCs early differentiation by modulating glycolysis (35). Induction of metabolism-associated genes (*PDK1*, *LDHA*, and *PYGL*) in ESCs by HIF-1α stabilization enhances glycolytic metabolism, which in turn results in ESC transition to epiblast stem cells. Second, Cited2 has been well characterized as a negative regulator of HIF-1 by competitive binding of HIF-1α to the CH1 domain of CBP/p300 (45). To examine whether hypoxia regulates glucose metabolism in *Cited2*$^{\Delta/-}$ EBs, the concentrations of glucose and lactate during differentiation under hypoxic conditions were measured. Compared with WT controls, *Cited2*$^{\Delta/-}$ EBs had a reduced rate of glucose consumption but the rate of lactate production was increased in *Cited2*$^{\Delta/-}$ EBs (Fig. 5, *B* and *C*), suggesting that a large proportion of glucose might be used for oxidative phosphorylation to supply ATP essential for differentiation in WT EBs. Indeed, measurement of glycolytic activity by the percentage of glucose converted to lactate revealed that ~40% of glucose was converted to lactate in WT EBs (Fig. 5*D*), whereas undifferentiated WT ESCs consumed ~80% of glucose for glycolysis, indicating that WT EBs experienced a metabolic switching during differentiation in agree-

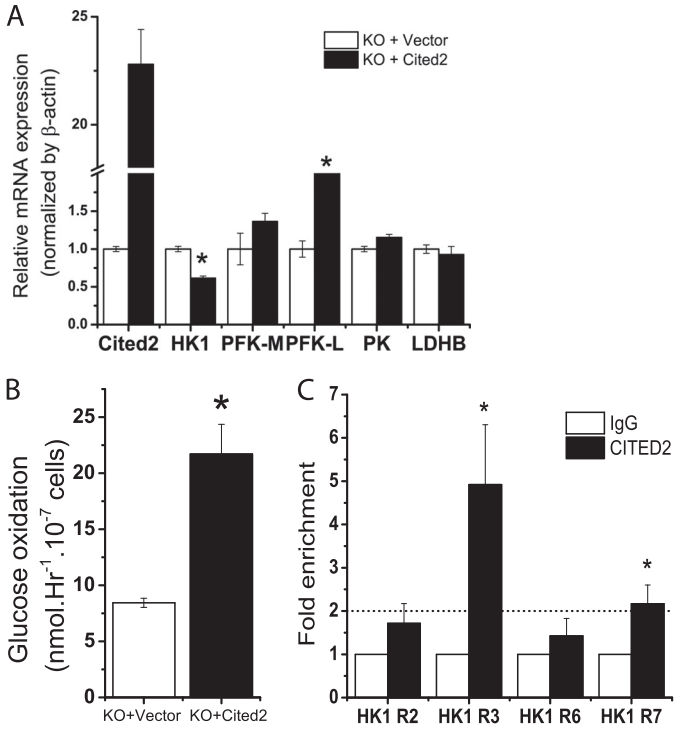

FIGURE 4. **Cited2-mediated regulation of metabolism-associated genes in undifferentiated ESCs.** *A*, effect of re-introduction of Cited2 to *Cited2*$^{\Delta/-}$ ESCs on metabolism-associated gene mRNA expression. *Cited2*$^{\Delta/-}$ ESCs were stably transfected with an empty vector or a Cited2 cDNA expression vector. Expression of *HK1*, *PFK1-M*, *PFK-L*, *PK*, and *LDHB* mRNA in WT and *Cited2*$^{\Delta/-}$ ESCs was determined by quantitative RT-PCR and normalized by internal control β-actin. Data from two independent experiments are presented. *B*, reintroduction of Cited2 increased glucose oxidation in *Cited2*$^{\Delta/-}$ ESCs. *C*, recruitment of Cited2 protein to the *HK1* gene promoter determined by ChIP-PCR. Enrichment of Cited2 protein on the *HK1* promoter was normalized to IgG controls set as 1.0. Experiments were repeated 4–5 times and data expressed as the mean ± S.E. *, $p < 0.05$ compared with *Cited2*$^{\Delta/-}$ ESCs controls.

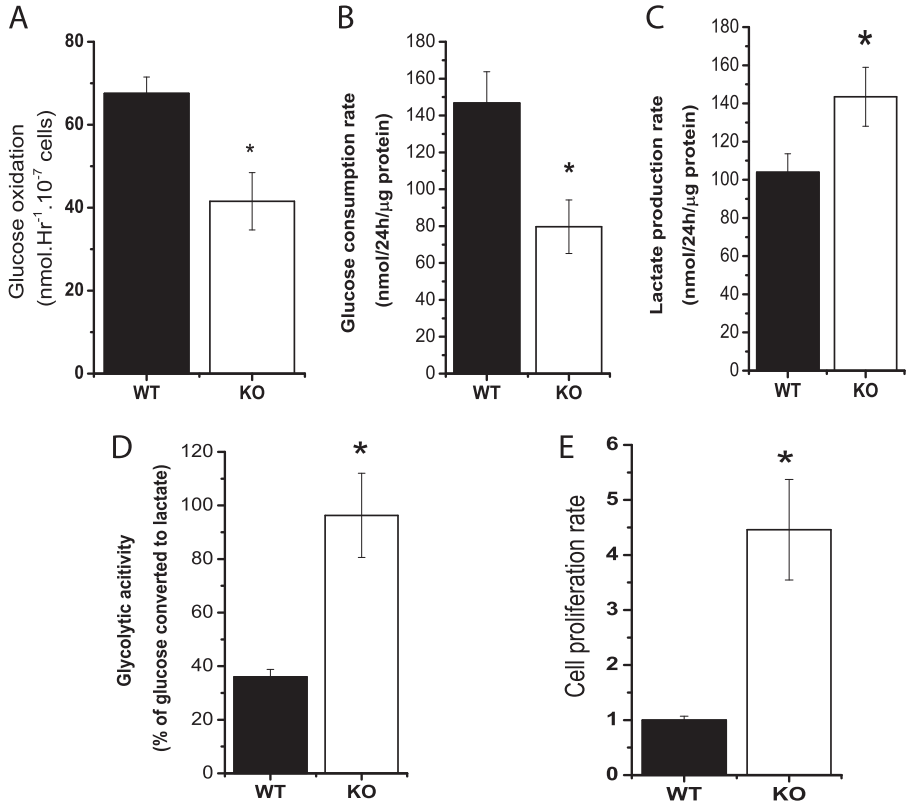

FIGURE 5. **Deletion of *Cited2* in ESCs results in a reduced rate of glucose oxidation via the TCA cycle and an increased glycolytic activity during differentiation.** *A,* glucose oxidation in WT and *Cited2*$^{\Delta/-}$ EBs induced to cardiomyocyte differentiation. WT and *Cited2*$^{\Delta/-}$ ESCs were induced to differentiate to cardiomyocytes using the hanging-drop method; at day 5 the conversion of [U-^{14}C]glucose to CO_2 was determined. Two independent experiments were performed and data are presented as the mean ± S.E. *B–D*, determination of the rate of glucose consumption, lactate production, and glycolytic activity in WT and *Cited2*$^{\Delta/-}$ EBs during hypoxic differentiation. Three thousand undifferentiated ESCs were induced to differentiation in 1 ml of methylcellulose-based semisolid media under hypoxia (2.5%). The concentrations of glucose and lactate in the media were measured as described under "Experimental Procedures" for determination the rate of glucose consumption (*B*), lactate production (*C*), and glycolytic activity (*D*). Data are presented as mean ± S.E., $n = 3$. *E,* enhanced glycolytic activity correlates with an increased rate of proliferation of *Cited2*$^{\Delta/-}$ EBs during hypoxia. Cell numbers were counted and normalized to the WT group set as 1.0. *, $p < 0.05$ compared with WT controls.

ment with a previous study (46). In contrast, the majority of glucose (~95%) was still converted to lactate in *Cited2*$^{\Delta/-}$ EBs (Fig. 5*D*) as did in undifferentiated *Cited2*$^{\Delta/-}$ ESCs. Furthermore, ~2.5-fold increase in glycolytic activity resulted in ~4.5-fold higher cell proliferation rate in *Cited2*$^{\Delta/-}$ EBs (Fig. 5*E*). These results suggest that deletion of *Cited2* results in reduced glucose oxidation and enhanced glycolytic activity in both undifferentiated and differentiating ESCs.

We next tested whether metabolic defects of *Cited2*$^{\Delta/-}$ ESCs affects proper ESC differentiation under hypoxia by examining the expression of the pluripotency gene (*Oct4*) and differentiation genes (*Fgf5*, *T*, *Gata-6*, and *Cdx2*) (47). *Oct4* gene expression was gradually reduced in differentiating WT ESCs during hypoxia, indicative of proper ESC differentiation (Fig. 6*A*). In contrast, the expression of *Oct4* remained high in differentiating *Cited2*$^{\Delta/-}$ ESCs (Fig. 6*A*), which is consistent with our previous report that Cited2 regulates expression of the Oct4 gene to control ESC differentiation during normoxia (22). *Fgf5*, a primitive epiblast marker for ESC differentiation, was induced in WT EBs at day 3.5 and the expression level was gradually reduced at EB days 4.5 and 5.5. Compared with WT controls, *Fgf5* mRNA was induced to similar levels at EB day 3.5, whereas there was increased induction of *Fgf5* at EB days 4.5 and 5.5 in *Cited2*$^{\Delta/-}$ EBs. Induction of *T* and *Gata-6*, a mesoderm marker and an endoderm marker, respectively, was significantly reduced in *Cited2*$^{\Delta/-}$ EBs at days 3.5 and 4.5 as compared with WT controls (Fig. 6*A*). *Cited2*$^{\Delta/-}$ EBs had a lower level of expression of *Cdx2*, a trophectoderm marker, at EB days 3.5 and 4.5, whereas there was a higher induction at EB day 5.5 compared with WT controls (Fig. 6*A*). Because *Cited2*$^{\Delta/-}$ EBs had a defective induction of the mesoderm marker *T* gene, we performed a colony formation unit (CFU) assay to examine whether differentiation to hematopoietic cells, a *bona fide* mesoderm lineage, is affected. Indeed, cfu-erythroid (CFU-E), CFU-granulocyte-macrophage (CFU-GM), and CFU-mixed colonies were significantly reduced in *Cited2*$^{\Delta/-}$ ESCs under hypoxic conditions (Fig. 6*B*). Collectively, we show that *Cited2*$^{\Delta/-}$ ESCs have impaired differentiation during hypoxia, as evidenced by their inability to down-regulate pluripotency genes, an improper induction of lineage marker genes, and defective hematopoietic cell differentiation. Taken together, increased glycolytic activity, reduced glucose oxidation, and the inability to switch off glycolysis in differentiating *Cited2*$^{\Delta/-}$ ESCs may contribute to defective cell lineage specification.

HIF-1 Regulates Expression of Differentiation Genes in Cited2$^{\Delta/-}$ *ESCs*—Because *Cited2*$^{\Delta/-}$ ESCs during hypoxic differentiation had increased glycolytic activity and defective gene expression, we next investigated whether HIF-1α plays a major

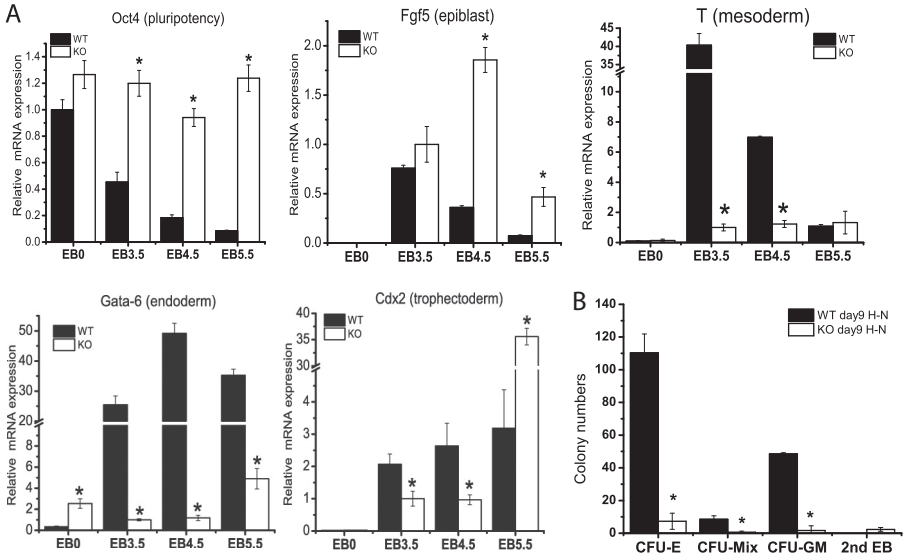

FIGURE 6. ***Cited2*$^{\Delta/-}$ embryoid bodies have impaired differentiation during hypoxia.** *A*, expression of genes controlling pluripotency and differentiation in WT and *Cited2*$^{\Delta/-}$ ESCs differentiating under hypoxia. To compare down-regulation of the Oct4 gene during differentiation, the level of *Oct4* mRNA in WT ESCs at day 0 (*EB0*) was set as 1.0. To monitor gene induction upon differentiation, mRNA expression of *Fgf5*, *T*, *Gata-6*, and *Cdx2* in *Cited2*$^{\Delta/-}$ EBs at day 3.5 was set as 1.0. *B*, *Cited2*$^{\Delta/-}$ ESCs have defective hematopoietic differentiation during hypoxia. Primary EBs differentiated in hypoxia for 9 days were re-suspended into a single cell suspension and a cell number equivalent to 50 WT EBs were re-plated in methylcellulose media, to support hematopoietic colony formation. The respective CFUs were counted 7 days after re-plating. The experiment was repeated 4 times in triplicate and one representative set of data are presented as the mean ± S.E. *, $p < 0.05$ compared with WT controls.

role in the initiation of differentiation program in *Cited2*$^{\Delta/-}$ ESCs. During hypoxic differentiation, a knockdown of HIF-1α (Fig. 7*A*) had no effect on the aberrant activation of *Oct4* mRNA in *Cited2*$^{\Delta/-}$ EBs (Fig. 7*B*). The expression of *Fgf5* was not affected at EB days 3.5 and 4.5 but was further up-regulated at EB day 5.5 in *Cited2*$^{\Delta/-}$ EBs with HIF-1α knockdown (Fig. 7*B*). Interestingly, defective induction of *T* and *Gata-6* mRNA in *Cited2*$^{\Delta/-}$ EBs was significantly resumed (Fig. 7*B*), whereas impaired trophectoderm marker *Cdx2* mRNA induction in *Cited2*$^{\Delta/-}$ EBs was not affected by HIF-1α knockdown (Fig. 7*B*). Thus, during hypoxic differentiation, a knockdown of HIF-1α modestly corrects the defective induction of the lineage differentiation genes *T* and *Gata-6* in *Cited2*$^{\Delta/-}$ EBs, indicating that HIF-1 is in part responsible for the defective mesoderm/endoderm differentiation in *Cited2*$^{\Delta/-}$ ESCs.

DISCUSSION

Cited2 is a well established transcription co-activator that competes with HIF-1α for binding to the CH1 domain of CBP/p300 (45). Accordingly, a knock-out of p300 or Cited2 in ESCs results in several similar phenotypes, such as delayed silencing of ESC pluripotency genes and defective hematopoietic differentiation (22, 48, 49). The role of p300 in ESC metabolism remains elusive. By monitoring glucose consumption and extracellular lactate production, we found that undifferentiated *Cited2*$^{\Delta/-}$ ESCs metabolize ~20% more glucose via aerobic glycolysis than WT counterparts, with a concomitant regulation of glycolysis-associated genes, such as *HK1* and *PFK1-L*. *HK1* is a target gene of Oct4 and HIF-1 (41, 50), two transcription factors previously shown to be modulated by Cited2 (8, 22). A ChIP assay indicated that Cited2 is recruited to the *HK1* gene promoter, further supporting the direct role of *Cited2* in coordinating HK1 expression and glucose metabolism. Cited2 deletion enhanced glycolysis and reduced glucose oxidation but did not affect mESC pluripotency and proliferation in undifferentiated ESCs, whereas these metabolic alternations impaired mESC differentiation through silence of pluripotency genes, activation of lineage specification genes, and cell proliferation.

During hypoxia, mammalian cells undergo glycolysis for energy production and HIF-1 is one of the major genes involved in this metabolic event (51). Cited2 competes with HIF-1α in binding to the CH1 domain of CBP/p300 and thus modulates key biological functions in heart, eye, and hematopoietic stem cells (8, 52–54). HIF-1 is responsible for controlling the rate of glycolysis in ESC lines with gain- or loss-of-function of HIF-1α. In *HIF-1*$\alpha^{-/-}$ ESCs, the induced expression of genes (including *Glut1*, *HK1*, *HK2*, *LDHA*, and *PGK1*) involved in the synthesis of ATP by the conversion of extracellular glucose to intracellular lactate was abrogated in response to hypoxia and hypoglycemic stresses (55, 56). Stabilization of HIF-1α in ESCs reduces mitochondrial respiration, whereas the rate of extracellular acidification is not significantly affected (35). Importantly, enhanced HIF-1 activity in ESCs is associated with the up-regulated expression of genes encoding glycolytic enzymes and enzymes involved in energy metabolism, which primes transition of mESC to epiblast stem cell (35). Targeted deletion of a histone deacetylase, Sirtuin-6 (*SIRT6*), in ESCs also results in increased glucose uptake and lactate production, whereas mitochondrial respiration is attenuated in *SIRT6*$^{-/-}$ ESCs (57). Mechanistically, the switch from glucose oxidation to CO_2 in the TCA cycle to glycolysis in *SIRT6*$^{-/-}$ ESCs is mediated by increased protein stability of HIF-1α, and the corresponding up-regulation of HIF-1 target genes, such as *LDHB*, *PDK4*, and *PDK1* (57). As a key regulator of metabolism, HIF-1 is an important transcription factor controlling multiple cell fate decisions, including mESC differentiation. During hypoxic differentiation, a knockdown of HIF-1α in *Cited2*$^{\Delta/-}$ EBs mod-

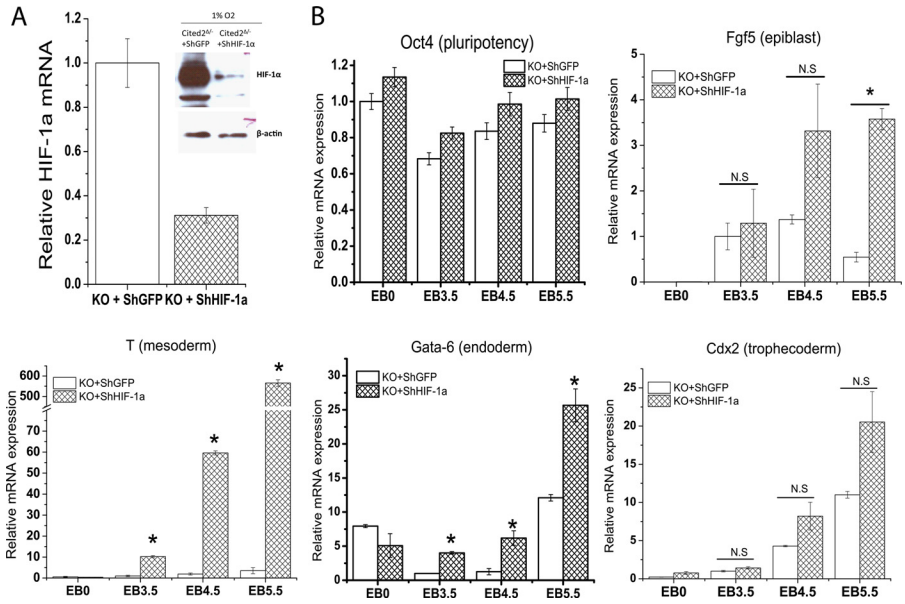

FIGURE 7. **Regulation of differentiation genes in *Cited2*$^{\Delta/-}$ ESCs by HIF-1.** *A*, knockdown of HIF-1α in *Cited2*$^{\Delta/-}$ ESCs. HIF-1α mRNA and protein expression in *Cited2*$^{\Delta/-}$ ESCs stably infected with lentivirus that expresses shGFP or shHIF-1α during hypoxia. *B*, effect of HIF-1α knockdown on the expression of pluripotency and differentiation genes in *Cited2*$^{\Delta/-}$ EBs during hypoxia. *Cited2*$^{\Delta/-}$ ESCs stably infected with lentivirus that expresses shGFP or shHIF-1α were induced to differentiate under hypoxia (2%) as described in the legend to Fig. 6*A* and respective gene expression was examined. *, mean ± S.E.: $p < 0.05$ compared with *Cited2*$^{\Delta/-}$ ESCs with shGFP controls.

estly induced the expression of the genes for *T* and *Gata-6*, which is consistent with reports that *T* and *Gata-6* are regulated by hypoxia (58, 59). The appearance of the mesoderm marker *T* gene after a HIF-1α knockdown in *Cited2*-deleted ESCs is also consistent with our previous study that HIF-1α down-regulation can partially rescue the defects in cardiac development (52). Our finding that dysregulated expression of pluripotency marker *Oct4*, epiblast marker *Fgf5*, and trophoectoderm marker *Cdx2* in *Cited2*$^{\Delta/-}$ EBs was not corrected by HIF-1α knockdown suggests several possibilities. 1) Hypoxic regulation in the EBs is dynamic and a critical time window for HIF-1α expression is thus essential for optimal ESC differentiation. 2) Fine tuning of the oxygen gradient in different regions of hypoxic EBs is crucial for ESC lineage specification. 3) HIF-1 independent mechanisms may contribute to these molecular events. Further investigation is warranted to distinguish these possibilities.

Mitochondria are the major energy hubs essential for ESC maintenance and proper differentiation. *Cited2*$^{\Delta/-}$ ESCs have swollen mitochondria, which are also found in ESCs in which *PINK1* (PTEN-induced putative kinase 1) has been deleted (60). Interestingly, both *Cited2* and *PINK1* genes are FOXO3a downstream targets (61). Enhanced glycolysis in IL-3-dependent hematopoietic cell lines with a knockdown of FOXO3a is sensitive to rapamycin and FOXO3α regulates glycolysis by modulating *TSC1* gene transcription (62). Expression of the gene for *Cited2* is regulated by FOXO3α (63), the mRNA of which is down-regulated by ~25% in *Cited2*$^{\Delta/-}$ ESCs, with no difference in *TSC1* mRNA expression (data not shown). The mechanisms responsible for similarities and differences of bio-energetic phenotypes in ESCs with deletions of these two FOXO3a target genes need to be further investigated.

Although oxidative phosphorylation is one of the typical features of ESC metabolism, the rate of oxygen consumption is extremely low in ESCs (15, 36). Our results demonstrated that ^{14}C-labeled acetate and glutamate oxidation in ESCs are barely detectable; permeabilized ESCs are not responsive to ADP addition, suggesting that mitochondria in ESCs are not as active as when they are at the homeostatic state. However, oxygen consumption in the ESCs is sensitive to rotenone treatment and this may reflect the potential ability of ESCs in responding to various differentiation cues and stress conditions; for example, treatment of ESCs with CCCP affects their differentiation (64). Furthermore, the knockdown of mitochondrial uncoupling protein 2 (UCP2) in human ESCs inhibits glycolysis, whereas the expression of ESC pluripotency markers, such as Oct4 and SSEA1, is not affected (32). Ectopic expression of UCP2 in human ESCs reduces glucose oxidation, impairs EB formation, and hampers early differentiation (32). Importantly, the mitochondrial metabolic stress-activated checkpoint in the control of ESC differentiation has been attributed to Ptpmt1 (protein-tyrosine phosphatase, mitochondrial 1), a mitochondrial PTEN-like phosphatidylinositol phosphate phosphatase (29); enhanced aerobic glycolysis, decreased oxygen consumption, compromised mitochondrial fusion/dynamics, and blocked differentiation was observed in Ptpmt1 knock-out ESCs (29). This implicates mitochondria as the key player in ESC differentiation and metabolic reprogramming, which may represent a unique way to modulate the fate of ESCs. To our knowledge, Cited2 is the first pro-differentiation gene whose deletion affects glucose oxidation and in turn ESC differentiation. Thus, our findings may provide a molecular basis for screening small molecules targeting Cited2 to modulate mitochondrial functions and control ESC pluripotency and differentiation.

The current investigation of the metabolic role of Cited2 also has significant implications for regenerative and clinical medicine. Metabolic reprogramming of glycolysis can greatly increase the efficiency of generating induced pluripotent stem

cells from somatic fibroblasts (21). It is thus imperative to investigate whether MEFs with a deletion in *Cited2* have an enhanced rate of glycolysis and reduced glucose oxidation via the TCA cycle, as noted with differentiating EBs with *Cited2* deletion. Small molecule inhibitors that target Cited2 and thus favor glycolysis may represent a novel method to increase induced pluripotent stem efficiency. On the other hand, embryonic stem cells and cancer cells are metabolically similar in that they utilize glycolysis to supply energy for proliferation. The metabolic changes in *Cited2*$^{\Delta/-}$ ESCs may also apply to cancer cells in which the gene for Cited2 has been silenced. In human hepatoma cells, Cited2, a direct effector of peroxisome proliferator-activated receptor γ, is down-regulated (65). Because many cancer initiating/stem cells reside in hypoxic regions of tissues and are resistant to routine therapy, it is plausible that alterations in the activity of Cited2 could be a potential therapeutic alternative to modulate metabolic processes, as suggested by the current study.

Acknowledgments—We thank Dr. Lawrence B. Gardner (Department of Pharmacology, Langone Medical Center, New York University) for providing HIF-1α shRNA plasmid, Dr. Xiangzi Han (Department of Pharmacology, Case Western Reserve University) for expertise on shRNA knockdown experiments, Michael Sramkoski at Case Comprehensive Cancer Center for help on flow cytometry and helpful suggestions from Drs. Xin Qi (Department of Physiology and Biophysics), Xuehuo Zeng (Department of Microbiology and Molecular Biology), Clark Distelhorst (Department of Medicine), and Anita Hjelmeland (Cleveland Clinic Lerner College of Medicine).

REFERENCES

1. Bamforth, S. D., Bragança, J., Eloranta, J. J., Murdoch, J. N., Marques, F. I., Kranc, K. R., Farza, H., Henderson, D. J., Hurst, H. C., and Bhattacharya, S. (2001) Cardiac malformations, adrenal agenesis, neural crest defects and exencephaly in mice lacking Cited2, a new Tfap2 co-activator. *Nat. Genet.* **29,** 469–474
2. Qu, X., Lam, E., Doughman, Y. Q., Chen, Y., Chou, Y. T., Lam, M., Turakhia, M., Dunwoodie, S. L., Watanabe, M., Xu, B., Duncan, S. A., and Yang, Y. C. (2007) Cited2, a coactivator of HNF4α, is essential for liver development. *EMBO J.* **26,** 4445–4456
3. Yin, Z., Haynie, J., Yang, X., Han, B., Kiatchoosakun, S., Restivo, J., Yuan, S., Prabhakar, N. R., Herrup, K., Conlon, R. A., Hoit, B. D., Watanabe, M., and Yang, Y. C. (2002) The essential role of Cited2, a negative regulator for HIF-1α, in heart development and neurulation. *Proc. Natl. Acad. Sci. U.S.A.* **99,** 10488–10493
4. Weninger, W. J., Lopes Floro, K., Bennett, M. B., Withington, S. L., Preis, J. I., Barbera, J. P., Mohun, T. J., and Dunwoodie, S. L. (2005) Cited2 is required both for heart morphogenesis and establishment of the left-right axis in mouse development. *Development* **132,** 1337–1348
5. Simsek, T., Kocabas, F., Zheng, J., Deberardinis, R. J., Mahmoud, A. I., Olson, E. N., Schneider, J. W., Zhang, C. C., and Sadek, H. A. (2010) The distinct metabolic profile of hematopoietic stem cells reflects their location in a hypoxic niche. *Cell Stem Cell* **7,** 380–390
6. Ito, K., Carracedo, A., Weiss, D., Arai, F., Ala, U., Avigan, D. E., Schafer, Z. T., Evans, R. M., Suda, T., Lee, C. H., and Pandolfi, P. P. (2012) A PML-PPAR-δ pathway for fatty acid oxidation regulates hematopoietic stem cell maintenance. *Nat. Med.* **18,** 1350–1358
7. Kranc, K. R., Schepers, H., Rodrigues, N. P., Bamforth, S., Villadsen, E., Ferry, H., Bouriez-Jones, T., Sigvardsson, M., Bhattacharya, S., Jacobsen, S. E., and Enver, T. (2009) Cited2 is an essential regulator of adult hematopoietic stem cells. *Cell Stem Cell* **5,** 659–665
8. Du, J., Chen, Y., Li, Q., Han, X., Cheng, C., Wang, Z., Danielpour, D., Dunwoodie, S. L., Bunting, K. D., and Yang, Y. C. (2012) HIF-1α deletion partially rescues defects of hematopoietic stem cell quiescence caused by Cited2 deficiency. *Blood* **119,** 2789–2798
9. Sakai, M., Matsumoto, M., Tujimura, T., Yongheng, C., Noguchi, T., Inagaki, K., Inoue, H., Hosooka, T., Takazawa, K., Kido, Y., Yasuda, K., Hiramatsu, R., Matsuki, Y., and Kasuga, M. (2012) CITED2 links hormonal signaling to PGC-1α acetylation in the regulation of gluconeogenesis. *Nat. Med.* **18,** 612–617
10. Coletta, D. K., Balas, B., Chavez, A. O., Baig, M., Abdul-Ghani, M., Kashyap, S. R., Folli, F., Tripathy, D., Mandarino, L. J., Cornell, J. E., Defronzo, R. A., and Jenkinson, C. P. (2008) Effect of acute physiological hyperinsulinemia on gene expression in human skeletal muscle *in vivo*. *Am. J. Physiol. Endocrinol Metab.* **294,** E910–917
11. Duggirala, R., Blangero, J., Almasy, L., Arya, R., Dyer, T. D., Williams, K. L., Leach, R. J., O'Connell, P., and Stern, M. P. (2001) A major locus for fasting insulin concentrations and insulin resistance on chromosome 6q with strong pleiotropic effects on obesity-related phenotypes in nondiabetic Mexican Americans. *Am. J. Hum. Genet.* **68,** 1149–1164
12. Asmann, Y. W., Stump, C. S., Short, K. R., Coenen-Schimke, J. M., Guo, Z., Bigelow, M. L., and Nair, K. S. (2006) Skeletal muscle mitochondrial functions, mitochondrial DNA copy numbers, and gene transcript profiles in type 2 diabetic and nondiabetic subjects at equal levels of low or high insulin and euglycemia. *Diabetes* **55,** 3309–3319
13. Wang, J., Alexander, P., Wu, L., Hammer, R., Cleaver, O., and McKnight, S. L. (2009) Dependence of mouse embryonic stem cells on threonine catabolism. *Science* **325,** 435–439
14. Johnson, M. T., Mahmood, S., and Patel, M. S. (2003) Intermediary metabolism and energetics during murine early embryogenesis. *J. Biol. Chem.* **278,** 31457–31460
15. Kondoh, H., Lleonart, M. E., Nakashima, Y., Yokode, M., Tanaka, M., Bernard, D., Gil, J., and Beach, D. (2007) A high glycolytic flux supports the proliferative potential of murine embryonic stem cells. *Antioxid. Redox Signal.* **9,** 293–299
16. Zhu, H., Shyh-Chang, N., Segrè, A. V., Shinoda, G., Shah, S. P., Einhorn, W. S., Takeuchi, A., Engreitz, J. M., Hagan, J. P., Kharas, M. G., Urbach, A., Thornton, J. E., Triboulet, R., Gregory, R. I., DIAGRAM Consortium, MAGIC Investigators, Altshuler, D., and Daley, G. Q. (2011) The Lin28/let-7 axis regulates glucose metabolism. *Cell* **147,** 81–94
17. Fan, Y., Dickman, K. G., and Zong, W. X. (2010) Akt and c-Myc differentially activate cellular metabolic programs and prime cells to bioenergetic inhibition. *J. Biol. Chem.* **285,** 7324–7333
18. Folmes, C. D., Martinez-Fernandez, A., Faustino, R. S., Yamada, S., Perez-Terzic, C., Nelson, T. J., and Terzic, A. (2013) Nuclear reprogramming with c-Myc potentiates glycolytic capacity of derived induced pluripotent stem cells. *J. Cardiovasc. Transl. Res.* **6,** 10–21
19. Chung, S., Dzeja, P. P., Faustino, R. S., Perez-Terzic, C., Behfar, A., and Terzic, A. (2007) Mitochondrial oxidative metabolism is required for the cardiac differentiation of stem cells. *Nat. Clin. Pract. Cardiovasc. Med.* **4,** S60–S67
20. Folmes, C. D., Dzeja, P. P., Nelson, T. J., and Terzic, A. (2012) Metabolic plasticity in stem cell homeostasis and differentiation. *Cell Stem Cell* **11,** 596–606
21. Folmes, C. D., Nelson, T. J., Martinez-Fernandez, A., Arrell, D. K., Lindor, J. Z., Dzeja, P. P., Ikeda, Y., Perez-Terzic, C., and Terzic, A. (2011) Somatic oxidative bioenergetics transitions into pluripotency-dependent glycolysis to facilitate nuclear reprogramming. *Cell Metab.* **14,** 264–271
22. Li, Q., Ramírez-Bergeron, D. L., Dunwoodie, S. L., and Yang, Y. C. (2012) Cited2 gene controls pluripotency and cardiomyocyte differentiation of murine embryonic stem cells through *Oct4* gene. *J. Biol. Chem.* **287,** 29088–29100
23. Yang, S. H., Kalkan, T., Morrisroe, C., Smith, A., and Sharrocks, A. D. (2012) A genome-wide RNAi screen reveals MAP kinase phosphatases as key ERK pathway regulators during embryonic stem cell differentiation. *PLoS Genet.* **8,** e1003112
24. Han, Y., Kuang, S. Z., Gomer, A., and Ramirez-Bergeron, D. L. (2010) Hypoxia influences the vascular expansion and differentiation of embryonic stem cell cultures through the temporal expression of vascular endothelial growth factor receptors in an ARNT-dependent manner. *Stem*

Cells **28,** 799–809
25. Ballard, F. J., and Hanson, R. W. (1969) Measurement of adipose-tissue metabolites *in vivo*. *Biochem. J.* **112,** 195–202
26. Slein, M. W. (1965) *Methods of Enzymatic Analysis*, Academic Press Inc., New York
27. Hohorst, H. J. (1965) *Methods of Enzymatic Analysis*, Academic Press Inc., New York
28. Jomain, M., and Hanson, R. W. (1969) Dietary protein and the control of fatty acid synthesis in rat adipose tissue. *J. Lipid Res.* **10,** 674–680
29. Shen, J., Liu, X., Yu, W. M., Liu, J., Nibbelink, M. G., Guo, C., Finkel, T., and Qu, C. K. (2011) A critical role of mitochondrial phosphatase Ptpmt1 in embryogenesis reveals a mitochondrial metabolic stress-induced differentiation checkpoint in embryonic stem cells. *Mol. Cell. Biol.* **31,** 4902–4916
30. Gnaiger, E., Kuznetsov, A.V., Schneeberger, S., Seiler, R., Brandacher, G., Steurer, W., and Margreiter, R. (2000) *Mitochondria in the Cold*, Springer, Berlin
31. Ye, F., Lemieux, H., Hoppel, C. L., Hanson, R. W., Hakimi, P., Croniger, C. M., Puchowicz, M., Anderson, V. E., Fujioka, H., and Stavnezer, E. (2011) Peroxisome proliferator-activated receptor γ (PPARγ) mediates a Ski oncogene-induced shift from glycolysis to oxidative energy metabolism. *J. Biol. Chem.* **286,** 40013–40024
32. Zhang, J., Khvorostov, I., Hong, J. S., Oktay, Y., Vergnes, L., Nuebel, E., Wahjudi, P. N., Setoguchi, K., Wang, G., Do, A., Jung, H. J., McCaffery, J. M., Kurland, I. J., Reue, K., Lee, W. N., Koehler, C. M., and Teitell, M. A. (2011) UCP2 regulates energy metabolism and differentiation potential of human pluripotent stem cells. *EMBO J.* **30,** 4860–4873
33. Nemetski, S. M., and Gardner, L. B. (2007) Hypoxic regulation of Id-1 and activation of the unfolded protein response are aberrant in neuroblastoma. *J. Biol. Chem.* **282,** 240–248
34. Lee, T. I., Johnstone, S. E., and Young, R. A. (2006) Chromatin immunoprecipitation and microarray-based analysis of protein location. *Nat. Protoc.* **1,** 729–748
35. Zhou, W., Choi, M., Margineantu, D., Margaretha, L., Hesson, J., Cavanaugh, C., Blau, C. A., Horwitz, M. S., Hockenbery, D., Ware, C., and Ruohola-Baker, H. (2012) HIF1alpha induced switch from bivalent to exclusively glycolytic metabolism during ESC-to-EpiSC/hESC transition. *EMBO J.* **31,** 2103–2116
36. Wilkerson, D. C., and Sankar, U. (2011) Mitochondria, A sulfhydryl oxidase and fission GTPase connect mitochondrial dynamics with pluripotency in embryonic stem cells. *Int. J. Biochem. Cell Biol.* **43,** 1252–1256
37. Peng, T. I., and Jou, M. J. (2004) Mitochondrial swelling and generation of reactive oxygen species induced by photoirradiation are heterogeneously distributed. *Ann. N.Y. Acad. Sci.* **1011,** 112–122
38. Tamai, S., Iida, H., Yokota, S., Sayano, T., Kiguchiya, S., Ishihara, N., Hayashi, J., Mihara, K., and Oka, T. (2008) Characterization of the mitochondrial protein LETM1, which maintains the mitochondrial tubular shapes and interacts with the AAA-ATPase BCS1L. *J. Cell Sci.* **121,** 2588–2600
39. Papanicolaou, K. N., Kikuchi, R., Ngoh, G. A., Coughlan, K. A., Dominguez, I., Stanley, W. C., and Walsh, K. (2012) Mitofusins 1 and 2 are essential for postnatal metabolic remodeling in heart. *Circ. Res.* **111,** 1012–1026
40. Zhou, J., Freeman, T. A., Ahmad, F., Shang, X., Mangano, E., Gao, E., Farber, J., Wang, Y., Ma, X. L., Woodgett, J., Vagnozzi, R. J., Lal, H., and Force, T. (2013) GSK-3α is a central regulator of age-related pathologies in mice. *J. Clin. Invest.,* in press
41. Kang, J., Shakya, A., and Tantin, D. (2009) Stem cells, stress, metabolism and cancer. A drama in two Octs. *Trends Biochem. Sci.* **34,** 491–499
42. McCleland, M. L., Adler, A. S., Shang, Y., Hunsaker, T., Truong, T., Peterson, D., Torres, E., Li, L., Haley, B., Stephan, J. P., Belvin, M., Hatzivassiliou, G., Blackwood, E. M., Corson, L., Evangelista, M., Zha, J., and Firestein, R. (2012) An integrated genomic screen identifies LDHB as an essential gene for triple-negative breast cancer. *Cancer Res.* **72,** 5812–5823
43. Sun, Q., Chen, X., Ma, J., Peng, H., Wang, F., Zha, X., Wang, Y., Jing, Y., Yang, H., Chen, R., Chang, L., Zhang, Y., Goto, J., Onda, H., Chen, T., Wang, M. R., Lu, Y., You, H., Kwiatkowski, D., and Zhang, H. (2011) Mammalian target of rapamycin up-regulation of pyruvate kinase isoenzyme type M2 is critical for aerobic glycolysis and tumor growth. *Proc. Natl. Acad. Sci. U.S.A.* **108,** 4129–4134
44. Zha, X., Wang, F., Wang, Y., He, S., Jing, Y., Wu, X., and Zhang, H. (2011) Lactate dehydrogenase B is critical for hyperactive mTOR-mediated tumorigenesis. *Cancer Res.* **71,** 13–18
45. Bhattacharya, S., Michels, C. L., Leung, M. K., Arany, Z. P., Kung, A. L., and Livingston, D. M. (1999) Functional role of p35srj, a novel p300/CBP binding protein, during transactivation by HIF-1. *Genes Dev.* **13,** 64–75
46. Song, J., Saha, S., Gokulrangan, G., Tesar, P. J., and Ewing, R. M. (2012) DNA and chromatin modification networks distinguish stem cell pluripotent ground states. *Mol. Cell. Proteomics* **11,** 1036–1047
47. Ou, X., Chae, H. D., Wang, R. H., Shelley, W. C., Cooper, S., Taylor, T., Kim, Y. J., Deng, C. X., Yoder, M. C., and Broxmeyer, H. E. (2011) SIRT1 deficiency compromises mouse embryonic stem cell hematopoietic differentiation, and embryonic and adult hematopoiesis in the mouse. *Blood* **117,** 440–450
48. Zhong, X., and Jin, Y. (2009) Critical roles of coactivator p300 in mouse embryonic stem cell differentiation and Nanog expression. *J. Biol. Chem.* **284,** 9168–9175
49. Rebel, V. I., Kung, A. L., Tanner, E. A., Yang, H., Bronson, R. T., and Livingston, D. M. (2002) Distinct roles for CREB-binding protein and p300 in hematopoietic stem cell self-renewal. *Proc. Natl. Acad. Sci. U.S.A.* **99,** 14789–14794
50. Luo, F., Liu, X., Yan, N., Li, S., Cao, G., Cheng, Q., Xia, Q., and Wang, H. (2006) Hypoxia-inducible transcription factor-1α promotes hypoxia-induced A549 apoptosis via a mechanism that involves the glycolysis pathway. *BMC Cancer* **6,** 26
51. DeBerardinis, R. J., Lum, J. J., Hatzivassiliou, G., and Thompson, C. B. (2008) The biology of cancer. Metabolic reprogramming fuels cell growth and proliferation. *Cell Metab.* **7,** 11–20
52. Xu, B., Doughman, Y., Turakhia, M., Jiang, W., Landsettle, C. E., Agani, F. H., Semenza, G. L., Watanabe, M., and Yang, Y. C. (2007) Partial rescue of defects in Cited2-deficient embryos by HIF-1α heterozygosity. *Dev. Biol.* **301,** 130–140
53. Chen, Y., Doughman, Y. Q., Gu, S., Jarrell, A., Aota, S., Cvekl, A., Watanabe, M., Dunwoodie, S. L., Johnson, R. S., van Heyningen, V., Kleinjan, D. A., Beebe, D. C., and Yang, Y. C. (2008) Cited2 is required for the proper formation of the hyaloid vasculature and for lens morphogenesis. *Development* **135,** 2939–2948
54. Huang, T. Q., Wang, Y., Ebrahem, Q., Chen, Y., Cheng, C., Doughman, Y. Q., Watanabe, M., Dunwoodie, S. L., and Yang, Y. C. (2012) Deletion of HIF-1α partially rescues the abnormal hyaloid vascular system in Cited2 conditional knockout mouse eyes. *Mol. Vis.* **18,** 1260–1270
55. Ryan, H. E., Lo, J., and Johnson, R. S. (1998) HIF-1 alpha is required for solid tumor formation and embryonic vascularization. *EMBO J.* **17,** 3005–3015
56. Chavez, J. C., Baranova, O., Lin, J., and Pichiule, P. (2006) The transcriptional activator hypoxia inducible factor 2 (HIF-2/EPAS-1) regulates the oxygen-dependent expression of erythropoietin in cortical astrocytes. *J. Neurosci.* **26,** 9471–9481
57. Zhong, L., D'Urso, A., Toiber, D., Sebastian, C., Henry, R. E., Vadysirisack, D. D., Guimaraes, A., Marinelli, B., Wikstrom, J. D., Nir, T., Clish, C. B., Vaitheesvaran, B., Iliopoulos, O., Kurland, I., Dor, Y., Weissleder, R., Shirihai, O. S., Ellisen, L. W., Espinosa, J. M., and Mostoslavsky, R. (2010) The histone deacetylase Sirt6 regulates glucose homeostasis via Hif1α. *Cell* **140,** 280–293
58. Nekanti, U., Dastidar, S., Venugopal, P., Totey, S., and Ta, M. (2010) Increased proliferation and analysis of differential gene expression in human Wharton's jelly-derived mesenchymal stromal cells under hypoxia. *Int. J. Biol. Sci.* **6,** 499–512
59. Ramírez-Bergeron, D. L., Runge, A., Dahl, K. D., Fehling, H. J., Keller, G., and Simon, M. C. (2004) Hypoxia affects mesoderm and enhances hemangioblast specification during early development. *Development* **131,** 4623–4634
60. Akundi, R. S., Zhi, L., Sullivan, P. G., and Bueler, H. (2012) Shared and cell type-specific mitochondrial defects and metabolic adaptations in primary cells from PINK1-deficient mice. *Neurodegener Dis.*, in press
61. Sengupta, A., Molkentin, J. D., Paik, J. H., DePinho, R. A., and Yutzey, K. E. (2011) FoxO transcription factors promote cardiomyocyte survival upon

induction of oxidative stress. *J. Biol. Chem.* **286,** 7468–7478
62. Khatri, S., Yepiskoposyan, H., Gallo, C. A., Tandon, P., and Plas, D. R. (2010) FOXO3a regulates glycolysis via transcriptional control of tumor suppressor TSC1. *J. Biol. Chem.* **285,** 15960–15965
63. Bakker, W. J., Harris, I. S., and Mak, T. W. (2007) FOXO3a is activated in response to hypoxic stress and inhibits HIF1-induced apoptosis via regulation of CITED2. *Mol. Cell* **28,** 941–953
64. Mandal, S., Lindgren, A. G., Srivastava, A. S., Clark, A. T., and Banerjee, U. (2011) Mitochondrial function controls proliferation and early differentiation potential of embryonic stem cells. *Stem Cells* **29,** 486–495
65. Cheung, K. F., Zhao, J., Hao, Y., Li, X., Lowe, A. W., Cheng, A. S., Sung, J. J., and Yu, J. (2013) CITED2 is a novel direct effector of peroxisome proliferator-activated receptor γ in suppressing hepatocellular carcinoma cell growth. *Cancer* **119,** 1217–1226